

Copper(I)-NHCs complexes: Synthesis, characterization and their inhibition against the biofilm formation of *Streptococcus mutans*



Ting Pan^{a,b}, Yinuo Wang^{a,b}, Feng-Shou Liu^c, Huancai Lin^{a,b,*}, Yan Zhou^{a,b,*}

^aHospital of Stomatology, Guanghua School of Stomatology, Sun Yat-Sen University, Guangzhou 510055, China

^bGuangdong Provincial Key Laboratory of Stomatology, Guangzhou 510055, China

^cSchool of Chemistry and Chemical Engineering, Guangdong Pharmaceutical University, Zhongshan 528458, China

ARTICLE INFO

Article history:

Received 9 December 2020

Accepted 10 January 2021

Available online 15 January 2021

Keywords:

Antibacterial

Streptococcus mutans

Oral biofilm

Dental caries

Copper *N*-heterocyclic carbenes

ABSTRACT

With the goal of developing high-efficiency oral antimicrobial agents to prevent *S. mutans* biofilm formation, a collection of copper(I)-*N*-heterocyclic carbenes (NHCs) complexes with different substitutions was synthesized and characterized. Their inhibitory activities of **Cu1**–**Cu7** were screened. It was found that **Cu1** provided significant excellent performance, which suggested that the less lipophilic and less sterically hindered copper complexes would be effective towards the bacteria. This study demonstrates the great potential of copper(I)-containing small molecule complexes as broad-spectrum inhibitors to treat oral bacteria, especially for diminishing *S. mutans* biofilm formation, which opens promising perspectives for the development of new metal-NHCs for controlling the biofilm formation associated with pathogens.

© 2021 Elsevier Ltd. All rights reserved.

1. Introduction

Since the first isolation of stable free *N*-heterocyclic carbenes (NHCs) by Arduengo, metal-NHC complexes have been recognized as a type of versatile compound in the fields of catalysis and organic synthesis [1–3]. In the past few years, metal-NHCs have received increasing attention in therapeutic and diagnostic medicines for their promising performance [4–8]. The key feature of NHC ligands is related to the strong σ -electron donor and weak π -electron acceptor in the carbene carbon, leading to a strong metal–carbon (M–C) bond. Therefore, the excellent stability of the metal complex would retard the cleavage of the M–C bond and therefore lower the high cytotoxicity of the metal ions. Moreover, the NHC ligands and metal complexes could be readily accessible through quite simple synthetic pathways, allowing for easy fine-tuning of the biological properties of these candidates [9].

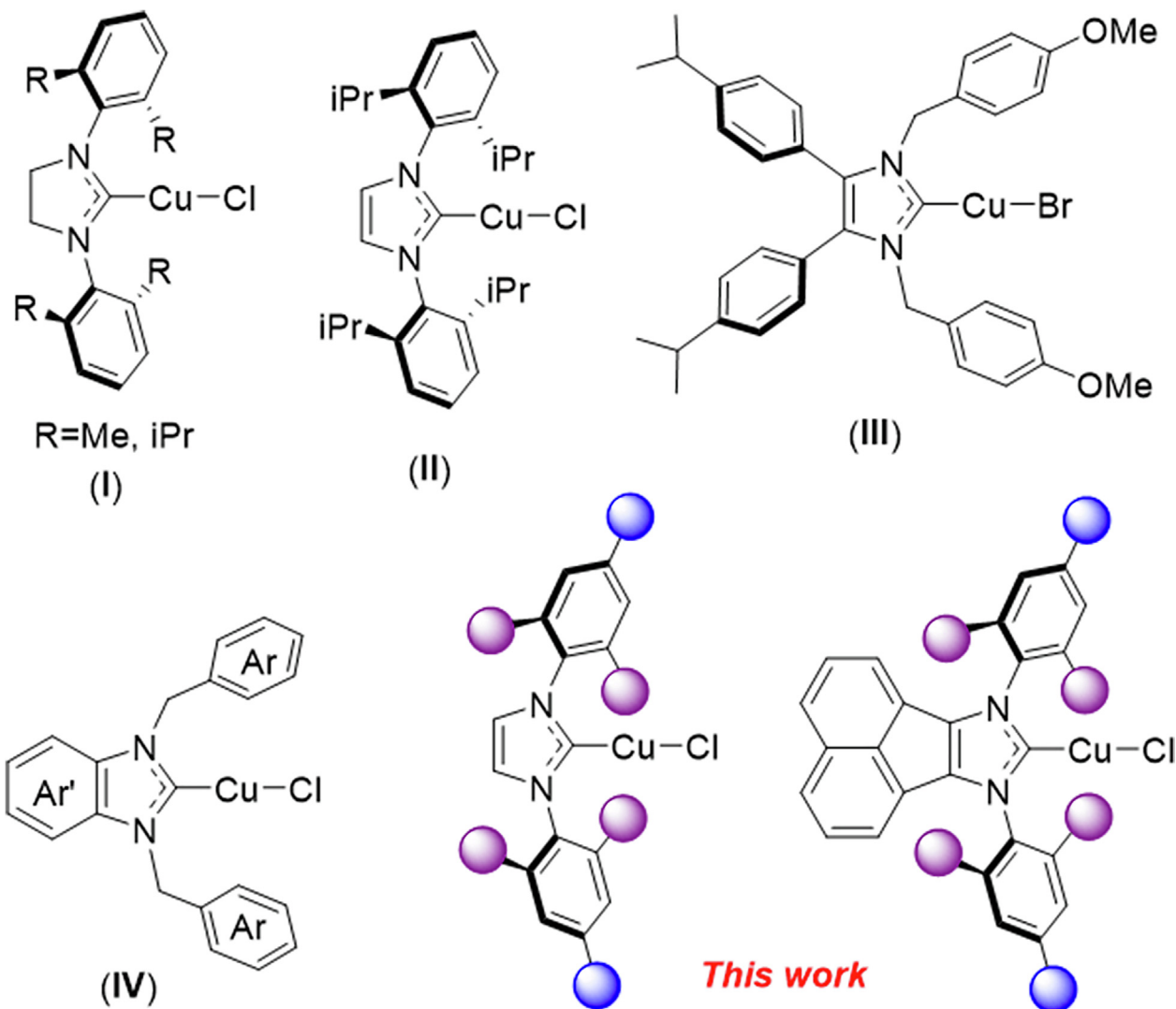
Until now, most efforts on the development of metal-NHCs have been focused on their antitumour activities using numerous metals, such as silver, gold, and copper [10–12]. In contrast, the antimicrobial properties of metal-NHCs are less explored and are mainly limited to the silver-NHCs [13–19]. The inhibition ability of the silver complexes is derived from the release of silver. However, sil-

ver-NHCs often suffer deactivation by light due to the relatively unstable silver–carbon bonds [20]. Thus, it is crucial to develop metal-NHCs with a strong coordination ability to maintain the stabilization of the metal complexes. On the other hand, copper-NHCs have been less explored (Scheme 1) even though copper-NHCs exhibit excellent stability towards air, moisture, and light [21–24]. Moreover, copper metal has long been recognized as an antimicrobial agent in drinking water treatment and transportation [25,26] and a copper-catalysed organic reaction could even be carried out inside mammalian cells with low cell toxicity [27]. Very recently, Roland revealed that copper-NHCs would be promising antibacterial agents, as they displayed excellent performance with regards to their inhibitory activity against *Listeria*, *Pseudomonas*, *Staphylococcus*, and *Escherichia* [28]. It was also revealed that copper-NHCs displayed comparable activity to silver-NHCs, which suggested that copper-NHCs could serve as potential antibacterial agent candidates. Moreover, Hamdi found that the benzimidazole-based copper-NHCs presented significant inhibitory activity against food-borne pathogens and clinical microorganisms [29]. Nevertheless, it remains to be determined whether copper-NHCs would be readily effective in the oral microbial environment.

Dental caries, the most common oral disease, is one of the most common chronic diseases in the world [30,31]. According to the statistical analysis of 328 diseases or injuries for 198 countries worldwide in 2016, the prevalence of dental caries was the most prevalent disease or injury [32]. *Streptococcus mutans* (*S. mutans*) is one of the major causative agents of dental caries. Its acid

* Corresponding authors at: Hospital of Stomatology, Guanghua School of Stomatology, Sun Yat-Sen University, Guangzhou 510055, China.

E-mail addresses: pant35@mail2.sysu.edu.cn (T. Pan), wyyinuo@mail2.sysu.edu.cn (Y. Wang), fengshou2004@126.com (F.-S. Liu), linhc@mail.sysu.edu.cn (H. Lin), zhouy75@mail.sysu.edu.cn (Y. Zhou).



Scheme 1. The biological activities of copper-*N*-heterocyclic carbenes (NHCs) complexes.

production, acid resistance, adhesion, ability to synthesize intracellular and extracellular polysaccharides (EPSs), and biofilm formation are closely related to the occurrence and development of caries [33,34]. In addition, certain pathogens can accelerate disease progression [35]. Therefore, it is extremely necessary to explore the effect of copper-NHCs on several strains of oral pathogenic bacteria, especially the inhibitory effect on *S. mutans* and its biofilm formation.

Inspired by the elegant works on the reported metal-NHCs as well as our previous study on the design of metal-NHCs [36–46] we describe herein the synthesis and characterization of a series of copper-NHCs and systematically investigate the relationship between the chemical structure and the performance. All of these complexes were screened for antibacterial activity against oral pathogens in vitro. We hypothesized that the synthesized complexes could have an effect on oral bacteria, especially *S. mutans*.

2. Experimental

2.1. Materials and methods

The NMR data of these copper-NHCs compounds were obtained on a Varian Mercury-Plus 400 MHz spectrometer at ambient tem-

perature with the decoupled nucleus using CDCl_3 as the solvent and referenced versus TMS as the standard. The X-ray diffraction data of a single crystal was obtained with the ω -2 θ scan mode on a Bruker SMART 1000 CCD diffractometer with graphite-monochromated Mo $K\alpha$ radiation ($\lambda = 0.71073 \text{ \AA}$) at 173 K for **Cu5**. The structure was solved using direct methods, and further refinement with full-matrix least-squares on F^2 was obtained with the SHELXTL program package. All non-hydrogen atoms were refined anisotropically. Hydrogen atoms were introduced in calculated positions with the displacement factors of the host carbon atoms. CCDC 2009625 (**Cu5**) contains the supplementary crystallographic data for this paper.

2.2. Synthetic procedure for carbene copper complexes

All of these copper complexes were synthesized according to the following procedures [47]. Among them, **Cu1** and **Cu3** were the previously reported compounds [48] while **Cu2** and **Cu4–Cu7** were reported for the first time.

A vial was charged with imidazolium salt (1.0 mmol), CuCl (1.0 mmol) and K_2CO_3 (2.0 mmol). Acetone (1.0 mL) was added into the mixture and stirred at 60 °C for 24 h. After that time, the solid was filtered and washed with dichloromethane. Then,

the filtrate was concentrated, and hexane (3.0 × 2.0 mL) was added. The solid precipitate of the desired product was dried under vacuum with yields in the range of 72–90%.

Cu2 was obtained in an 83% yield. ¹H NMR (400 MHz, CDCl₃) δ 7.37–7.30 (m, Ar-H, 8H), 7.27–7.22 (m, Ar-H, 5H), 7.19–7.13 (m, Ar-H, 8H), 7.07 (s, Ar-H, 2H), 6.94 (s, Ar-H, 4H), 5.54 (s, CH, 2H), 2.07 (s, CH₃, 12H). ¹³C NMR (101 MHz, CDCl₃) δ 178.9, 145.5, 143.2, 135.8, 134.7, 129.7, 129.5, 128.5, 126.5, 122.2, 56.4, 31.6, 22.6, 17.9, 14.1. Anal. Calc. for C₄₅H₄₀ClCuN₂: C, 76.36; H, 5.70; N, 3.96. Found: C: 76.21; H: 5.57; N: 3.90.

Cu4 was obtained in a 90% yield. ¹H NMR (400 MHz, CDCl₃) δ 7.78 (d, *J* = 8.1 Hz, Ar-H, 2H), 7.42 (dd, *J* = 8.3, 7.0 Hz, Ar-H, 2H), 7.10 (s, Ar-H, 4H), 7.05 (d, *J* = 6.7 Hz, Ar-H, 2H), 2.42 (s, 6H), 2.22 (s, 12H). ¹³C NMR (101 MHz, CDCl₃) δ 184.1, 139.6, 137.9, 134.4, 133.6, 130.6, 129.7, 129.6, 128.2, 127.7, 125.3, 120.9, 21.2, 17.9. Anal. Calc. for C₃₁H₂₈ClCuN₂: C, 70.58; H, 5.35; N, 5.31. Found: C: 70.32; H: 5.28; N: 5.24.

Cu5 was obtained in an 87% yield. ¹H NMR (400 MHz, CDCl₃) δ 7.81 (d, *J* = 8.3 Hz, Ar-H, 2H), 7.45 (dd, *J* = 8.2, 7.1 Hz, Ar-H, 2H), 7.39 (t, *J* = 7.5 Hz, Ar-H, 8H), 7.29 (t, *J* = 7.3 Hz, Ar-H, 4H), 7.24 (d, *J* = 7.2 Hz, Ar-H, 8H), 7.08–6.99 (m, Ar-H, 6H), 5.65 (s, CH, 2H), 2.20 (s, CH₃, 12H). ¹³C NMR (101 MHz, CDCl₃) δ 184.0, 145.6, 143.3, 137.9, 134.7, 134.5, 130.6, 130.0, 129.6, 129.5, 128.5, 128.3, 127.7, 126.5, 125.2, 120.9, 56.5, 18.1. Anal. Calc. for C₅₅H₄₄ClCuN₂: C, 79.40; H, 5.33; N, 3.37. Found: C: 79.24; H: 5.40; N: 3.32.

Cu6 was obtained in an 82% yield. ¹H NMR (400 MHz, CDCl₃) δ 7.79 (d, *J* = 8.3 Hz, Ar-H, 2H), 7.52 (t, *J* = 7.7 Hz, Ar-H, 2H), 7.46–7.31 (m, Ar-H, 6H), 6.98 (d, *J* = 6.9 Hz, Ar-H, 2H), 2.62 (q, *J* = 7.5 Hz, CH₂, 8H), 1.20 (t, *J* = 7.6 Hz, CH₃, 12H). ¹³C NMR (101 MHz, CDCl₃) δ 185.1, 140.8, 138.4, 134.9, 130.6, 130.3, 129.7, 128.3, 127.7, 127.4, 125.2, 121.0, 24.6, 15.0. Anal. Calc. for C₃₃H₃₂ClCuN₂: C, 71.34; H, 5.81; N, 5.04. Found: C: 71.25; H: 5.76; N: 4.93.

Cu7 was obtained in a 72% yield. ¹H NMR (400 MHz, CDCl₃) δ 7.80 (d, *J* = 8.2 Hz, Ar-H, 2H), 7.59 (t, *J* = 7.8 Hz, Ar-H, 2H), 7.46–7.39 (m, Ar-H, 6H), 7.01 (d, *J* = 6.9 Hz, Ar-H, 2H), 2.84 (dt, *J* = 13.8, 6.9 Hz, CH, 4H), 1.35 (d, *J* = 6.9 Hz, CH₃, 12H), 1.13 (d, *J* = 6.9 Hz, CH₃, 12H). ¹³C NMR (101 MHz, CDCl₃) δ 185.8, 145.6, 138.7, 133.1, 130.8, 129.8, 128.3, 127.8, 125.3, 124.5, 121.0, 28.9, 24.8, 23.7. Anal. Calc. for C₃₇H₄₀ClCuN₂: C, 72.65; H: 6.59; N: 4.58. Found: C: 72.57; H: 6.46; N: 4.51.

2.3. Antimicrobial activity assessment for carbene copper complexes

Before assessing the antimicrobial activity, the carbene copper complexes were dissolved in DMSO at an initial concentration of 10 mg/mL and stored at –20 °C.

2.3.1. Microorganism strains and growth conditions

A total of ten oral microorganisms were tested in this experiment, including seven gram-positive bacteria, two gram-negative bacteria and one fungus. *S. mutans* UA159, *Streptococcus gordonii* ATCC10558 (*S. gordonii*), *Streptococcus sanguis* ATCC10556 (*S. sanguis*), *Enterococcus faecalis* OG1RF (*E. faecalis*), *Lactobacillus casei* ATCC393 (*L. casei*), *Lactobacillus acidophilus* ATCC4356 (*L. acidophilus*), and *Actinomyces naeslundii* ATCC19039 (*A. naeslundii*) were grown in brain heart infusion (BHI), while *Candida albicans* SC5314 (*C. albicans*) was cultured in Sabouraud's dextrose broth (SDB, HKM, CHN). The other bacteria, including *Fusobacterium nucleatum* ATCC10953 (*F. nucleatum*) and *Actinobaculum actinomycetemcomitans* ATCC43717 (*A. a.*), were grown in a BHI solution supplemented with 0.5% yeast extract (Oxoid, UK), 0.04% L-cysteine (Sigma, USA), 5 µg/mL hemin (Macklin, CHN) and 1 µg/mL vitamin K1 (Aladdin, CHN). All bacterial strains were incubated in an anaerobic chamber (90% N₂, 5% H₂ and 5% CO₂, Thermo Scientific, MA,

USA) at 37 °C, while *C. albicans* reproduced under aerobic conditions with shaking at 200 rpm.

2.3.2. Minimum inhibitory concentrations (MICs) of the microorganisms

The MICs of the complexes against the ten microorganisms were determined by broth microdilution according to the guidelines of the Clinical and Laboratory Standards Institute [49]. In general, each microorganism was grown overnight at 37 °C to reach the mid-logarithmic phase. Cultures were diluted to 5 × 10⁵ CFU/mL in 96-well flat-bottom plates, whereas the fungus was diluted to 5 × 10³ CFU/mL. Serial dilutions of the drugs in microplates with the bacterial suspensions were incubated at 37 °C for 24 h with final drug concentrations ranging from 500 µg/mL to 0.49 µg/mL. The measured optical densities at 600 nm were combined with observations by the naked eye to evaluate the experimental results. Chlorhexidine gluconate was selected as the positive control. Microorganisms with the corresponding concentrations of DMSO and BHI (Difco, USA) broth medium served as the negative control and blank, respectively.

2.3.3. Time-kill assay

To study the killing kinetics of live bacteria, the effects of the complexes against *S. mutans* UA159 were determined. Briefly, previously grown *S. mutans* were diluted to 2 × 10⁷ CFU/mL and treated with copper-NHCs at the following concentrations: 1/2 MIC, MIC, and 2 MIC. Cultures without drug were used as the control group. At 0, 2, 4, 6, 8, 12 and 24 h post-inoculation, the cultures were diluted, spread onto BHI agar plates and incubated at 37 °C for 24 h to quantify the viable cell numbers.

2.3.4. Assessment of *S. mutans* biofilm biomass

The total biomass was investigated using crystal violet (CV) staining. *S. mutans* UA159 was suspended at a concentration of 2 × 10⁷ CFU/mL in 200 µL of BHI liquid medium with 1% sucrose (BHIS). After treatment with the complexes, the bacterial cell suspensions were used to form biofilms at 37 °C in approximately 5% CO₂ for a 24 h incubation period. Next, the cells were washed twice with sterile phosphate-buffered saline (PBS), fixed with 100% methyl alcohol for 15 min, and then the medium was replaced with 200 µL of 0.1% CV (Sigma, USA) for 15 min, after which the biofilm was washed with PBS to remove the residual dye. The adherent biomass stained with CV at the bottom of the plates was released with 200 µL of 95% ethanol. The absorbance values were measured at 595 nm using a microplate reader (Infinite 200, Tecan, SUI).

2.3.5. Evaluation of the metabolic activity of *S. mutans* biofilm

3-(4,5-Dimethylthiazol-2-yl)-2,5-diphenyltetrazolium bromide (MTT) was utilized to assess the metabolic activity of viable biofilm cells. MTT (Amresco, USA) powder was dissolved in PBS at a working concentration of 5 mg/mL under sterile conditions and stored at –20 °C. Biofilms were formed as described above. Then, 50 µL of MTT solution was added to each well, followed by incubation at 37 °C for 3 h in the dark. After removing the MTT solution, 100 µL of DMSO was used to dissolve the formazan, and then, the solution was transferred to a new plate. Wells containing no bacteria were used as blank controls, while wells without complexes served as negative controls. The absorbance values at 570 nm were detected. Metabolic activity = (OD_{test}–OD_{blank})/(OD_{negative} – OD_{blank}) × 100%.

2.3.6. LIVE/DEAD staining and confocal laser scanning microscopy (CLSM)

S. mutans UA159 was treated with complexes to establish biofilms on glass slides as described above. The 24 h biofilm was

mildly washed with PBS to remove planktonic bacteria and then stained with a LIVE/DEAD BacLight Bacterial Viability Kit (Invitrogen, USA) containing SYTO 9 and propidium iodide in the dark for 15 min. Excess dye was removed by washing the biofilm with PBS. A confocal laser scanning microscope (Zeiss, Germany) equipped with a 63 × oil immersion objective lens was applied to capture the images, which were then analysed by COMSTAT [50].

2.3.7. Measurement of extracellular polysaccharide (EPS) synthesis

S. mutans UA159 was inoculated in BHIS as previously described with an Alexa Fluor 647 (Invitrogen, USA)-labelled dextran conjugate. Similar to the procedures described, the biofilm was consequently washed with PBS and stained with SYTO 9 for 15 min. The sample images were captured by CLSM.

2.3.8. Scanning electron microscopy (SEM)

To observe morphological changes in the *S. mutans* UA159 biofilm treated with the complexes, bacterial cells were grown in BHIS and exposed to a screened working concentration at 37 °C. After 24 h, the samples were dehydrated in an ethanol series (30, 50, 70, 90, and 100%), critical point-dried with CO₂, coated with gold, and observed under a scanning electron microscope (Quanta 400F-FEI, Eindhoven, Netherlands).

2.3.9. In vitro cytotoxicity assay

The cytotoxicity of the complexes was assessed in human gingival epithelial cells (HGECS) using Cell Counting Kit-8 (CCK-8; Dojindo, Japan). HGECS were purchased from American Type Culture Collection (ATCC, Manassas, VA, USA) and cultured in defined keratinocyte serum-free medium (Gibco, USA). Assays were performed in 96-well plates with 10,000 cells per well. After incubation in a 5% CO₂ atmosphere for 24 h at 37 °C, the plates were washed with sterile PBS. Then, 100 μL of four gradient concentrations of each drug (0.98 μg/mL, 1.95 μg/mL, 3.91 μg/mL, and 7.81 μg/mL) in cell culture medium were added, respectively, followed by incubation for 10 min or 24 h. The negative control did not contain drug but did contain cells and medium, while the blank control was incubated with only cell culture medium. The medium was then completely removed and substituted with 100 μL of fresh cell culture medium and 10 μL of CCK-8 reagent. The plates were incubated for another 2 h, and then, the absorbance was measured at 450 nm with a microplate reader.

2.4. Statistical analysis

All experiments were repeated independently three times. One-way ANOVA was performed on multiple sets of samples to detect significant differences, followed by a Dunnett test. Two groups of samples were counted by an unpaired *t*-test. Statistical analysis was performed with GraphPad Prism version 7.0. A *P* value of <0.05 was considered significant.

3. Results

3.1. Synthesis and characterization of the copper-NHCs complexes

The copper-NHCs complexes were readily synthesized through the reaction of corresponding imidazolium chloride salt with CuCl in the presence of K₂CO₃, which afforded the desired copper complexes in high yields (Scheme 2). It is noteworthy that these copper complexes are rather stable towards air and moisture, and they were even stable in the DMSO solution for several months with no decomposition. The structures of these complexes were established by the ¹H NMR and ¹³C NMR, for which the resonance of C_{NHC} appeared in the range of 178.9–185.8 ppm and the low reso-

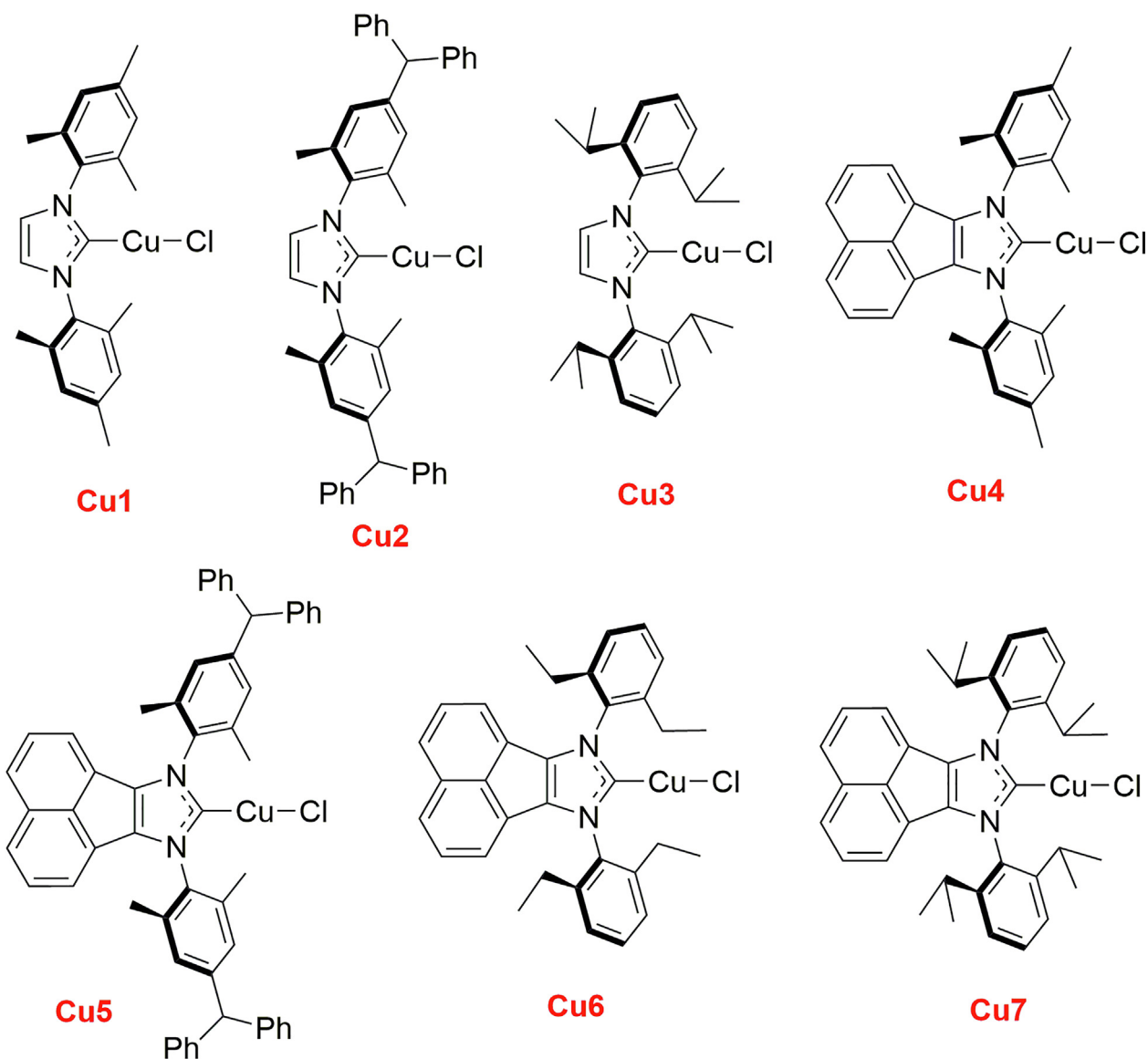
nance of the NCHN disappeared. Moreover, single crystals of **Cu5**, grown from the cosolvent of hexane and dimethylchloride, were further analysed by X-ray crystallographic analysis. The data collection and the parameters of the structural refinement are summarized in Table 1. The crystal of **Cu5** is triclinic with a space group of *P*-1: *Z* = 2, *a* = 13.2487(4) Å, *b* = 13.8207(5) Å, *c* = 15.5361(6) Å, α = 64.979(4)°, β = 66.129(3)°, and γ = 69.510(3)°. An ORTEP diagram is given in Fig. 1. The carbene ligand and chloride atoms coordinated towards the copper centre to form a slightly distorted linear complex with a bite angle of 179.43(7)°. It should be noted that the substituents of 2,6-dimethyl on *N*-aryl moieties are nearly perpendicular with the dihedral angles of 86.78 and 88.40°, respectively, which suggests that the axial steric environment would exert an impact on the metal ion and further play a key role in its antibacterial properties. Moreover, the Cu–C_{NHC} and Cu–Cl bond lengths are similar to those of the previously reported copper-NHCs complexes, even though the steric environment around the copper centre varied [51,52].

3.2. Effectiveness against multiple oral pathogens

To preliminarily evaluate the antimicrobial activities of the synthesized complexes, we first determined the MICs of the copper complexes against *S. mutans* UA159. As shown in Table 2, the **Cu1** complex with 2,6-dimethyl groups on the *N*-moieties showed excellent biological activity with a low value of 1.95 μg/mL, which was comparable with the activity of the most commonly applied oral bacteriostatic agent, chlorhexidine. In contrast, **Cu2**, with 2,6-dimethyl groups and a bulky benzhydryl at the *para*-position of the *N* moieties, was also selected for evaluation, and moderate activity was found (31.25 μg/mL). Moreover, the more lipophilic **Cu3** complex, which contained 2,6-diisopropyl groups on the *N* moieties, had minor activity greater than 500 μg/mL against *S. mutans* UA159. Notably, **Cu3** was previously shown to display excellent inhibitory activity against *Listeria*, *Pseudomonas*, *Staphylococcus*, and *Escherichia* [28]. Subsequently, other copper complexes (**Cu4–Cu7**) with acenaphthyl backbones as well as different *N*-moieties were screened. It was suggested that their rapid decline in activity was due to their increase in sterility around the copper complexes.

With the primary results in hand, we selected **Cu1** and further examined the effect of **Cu1** on nine other oral pathogens including both gram-positive and gram-negative bacteria as well as fungi. As shown in Table 3, we were pleased to discover that the inhibition by **Cu1** was superior to that of chlorhexidine in six oral pathogenic bacteria, especially against *A. naeslundii* and *S. gordonii*, with MIC values of 0.49 μg/mL and 0.98 μg/mL, respectively. Moreover, the MIC of **Cu1** against *C. albicans* SC5314 was 3.91 μg/mL, which was lower than the MIC of 7.81 μg/mL shown by chlorhexidine (Table 3). Quite intriguingly, although broad-spectrum antibacterial activity against both gram-positive and gram-negative bacteria was observed, **Cu1** performed slightly better against gram-positive bacteria than gram-negative bacteria. **Cu1** showed prominent performance against *A. naeslundii*, *S. gordonii*, *S. sanguis*, *S. mutans* and *E. faecalis* (MIC 0.49–3.91 μg/mL), which are all gram-positive pathogens. However, the MICs against two gram-negative strains, *A. a* and *F. nucleatum*, were 1.95 μg/mL and 31.25 μg/mL, respectively.

Combining the data from Tables 2 and 3, **Cu1** showed the strongest inhibitory potency among the seven synthesized complexes. Notably, **Cu1** exhibited better activity against multiple bacterial strains in comparison with chlorhexidine. Inspired by the excellent biological performance of **Cu1**, further investigation on the inhibition of the growth of *S. mutans* UA159 was subsequently performed.



Scheme 2. The chemical structure of the copper-NHCs complexes.

3.3. Complexes inhibited the growth of *S. mutans* UA159

Fig. 2 shows the results of the time-kill assay of **Cu1** on *S. mutans*. The inhibitory behaviour obviously started after the addition of the drugs and remained for 24 h at the MIC. The viability of *S. mutans* displayed a steady reduction after treatment with **Cu1** at the MIC. At 2 MIC, the bactericidal effect was even more pronounced, with a substantial 99.85% reduction in bacterial cells after 2 h of treatment and complete killing by 4 h.

3.4. Inhibition of *S. mutans* UA159 biofilm formation by the complexes

CV assays were conducted to evaluate *S. mutans* biofilm formation under the influence of the complexes. Clearly, there was an obvious distinction in overall biomass in the treated groups compared with the drug-free group ($P < 0.001$). In the presence of **Cu1**, the biofilm biomass presented no significant changes at 1/2 MIC, but the biomass decreased sharply to nearly 2.45% at the MIC and could not be detected at concentrations corresponding to 2 MIC (Fig. 3a).

MTT assays were used for determining the metabolic activity of biofilms at the same concentrations of **Cu1** as mentioned above. The results of biofilm metabolism were consistent with the results of the CV experiment ($P < 0.001$). Compared to the control group, the biofilm metabolic activity decreased to 16.8% at the MIC after treatment with **Cu1** (Fig. 3b).

3.5. Alteration of the biofilm structure and morphology of *S. mutans* by the complexes

The biofilm of *S. mutans* treated with **Cu1** at the MIC for 24 h was investigated by CLSM (Fig. 4). In the presence of **Cu1**, the microarchitecture of the biofilm demonstrated a visibly sparse and loose distribution compared with that of the negative control, which consequently resulted in an apparent reduction in the total biofilm biomass ($P < 0.001$) and EPS synthesis ($P < 0.01$).

Consistent with the CLSM assay, no obvious biofilm formation was observed by SEM compared with the free drug group (Fig. 5). The addition of **Cu1** resulted in an atypical morphology of *S. mutans* with irregular edges and a significant reduction in

Table 1
Crystal data and structural refinement for Cu₅.

Identification code	Cu5
Empirical formula	C ₅₆ H ₄₆ Cl ₃ CuN ₂
Formula weight	916.84
Temperature/K	100.00(10)
Crystal system	Triclinic
Space group	P-1
a/Å	13.2487(4)
b/Å	13.8207(5)
c/Å	15.5361(6)
α/°	64.979(4)
β/°	66.129(3)
γ/°	69.510(3)
Volume/Å ³	2301.70(17)
Z	2
ρ _{calc} /cm ³	1.323
μ/mm ⁻¹	0.689
F(000)	952.0
Crystal size/mm ³	0.15 × 0.13 × 0.11
Radiation	MoKα (λ = 0.71073)
2θ range for data collection/°	6.634 to 59.228
Index ranges	-16 ≤ h ≤ 17, -18 ≤ k ≤ 17, -19 ≤ l ≤ 19
Reflections collected	19,481
Independent reflections	10,633 [R _{int} = 0.0312, R _{sigma} = 0.0583]
Data/restraints/parameters	10633/0/563
Goodness-of-fit on F ²	1.026
Final R indexes [I > = 2σ (I)]	R ₁ = 0.0479, wR ₂ = 0.1087
Final R indexes [all data]	R ₁ = 0.0630, wR ₂ = 0.1189
Largest diff. peak/hole/e Å ⁻³	0.44/-0.55

EPSs. Furthermore, the remaining bacterial cells had difficulty forming bacterial aggregates and the biofilm microarchitecture.

3.6. Exhibition of certain cytotoxicity on HGECs by the complexes

Next, we examined the cytotoxicity of **Cu1** on HGECs in order to investigate its biocompatibility (Fig. 6). Clearly, **Cu1** exhibited no significant inhibitory effects in a short period of time (10 min) below 1.95 μg/mL (MIC) ($p > 0.05$). Although the drug's toxicity

gradually increased with the increase of the concentration and extension of time (24 h), it is noticeable that **Cu1** still exhibited an effect, with approximately 50% viability of HGECs at the MIC ($P < 0.001$).

4. Discussion

Copper, as a crucial component for animals and microorganisms, has been widely researched for its redox capabilities and complexation potential [53]. Copper has been used as an antifungal or antibacterial agent for a long time, such as in the healthcare area to restrain bacteria in the water distribution network [54]. It has been proved that certain concentrations of copper ions can poison bacterial cells by inactivating key metal enzymes, especially those containing soluble iron and zinc [55,56]. On the other hand, it also has been widely studied that organic ligands combining with copper modulate the activity by neutralizing the electric charge of the copper ion, increasing the lipophilicity of the complex promoting transport through the cell membrane, intercalating to DNA or interacting non-covalently with proteins [57]. By chelating small molecular ligands, the antibacterial properties of copper can be selectively adjusted and even achieve the synergistic effects

Table 2
In vitro minimum inhibitory concentration assessment of synthetic complexes on planktonic *S. mutans* UA159.

MIC (μg/mL)	<i>S. mutans</i> UA159
Cu1	1.95
Cu2	31.25
Cu3	>500
Cu4	15.63
Cu5	>500
Cu6	>500
Cu7	>500
Chlorhexidine	0.49

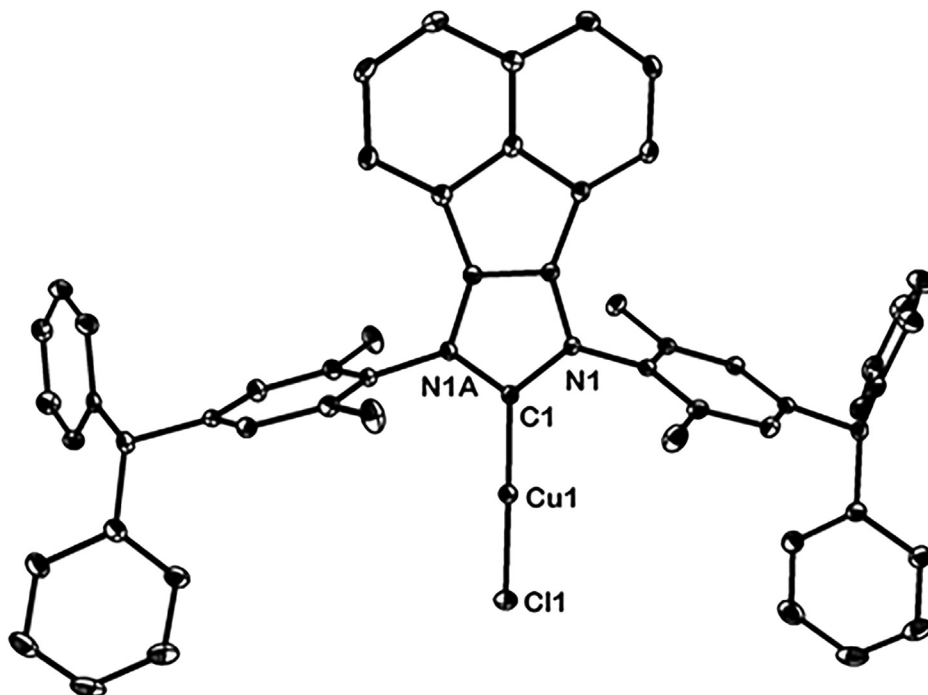


Fig. 1. Molecular structure of **Cu5** depicted in 30% thermal ellipsoids with the hydrogen atoms omitted for clarity. Selected bond distances (Å) and angles (°): Cu1–C1 1.873(2), N1–C1 1.374(3), N1A–C1 1.371(3), Cu1–Cl1 2.0989(7), Cu1–C1 1.873(2), C1–Cu1–Cl1 179.43(7).

observed with high-level antibacterials [53]. Albeit there are many well-known coordination complexes with copper, they are not fully appreciated with regards to copper-NHCs acting on the oral microbial environment. Therefore, we tested and reported a series of copper(I)-NHCs presenting effective inhibitory activity against

oral pathogens, especially free-living *S. mutans* and its biofilm form.

In the present study, it was highlighted that the much less lipophilic compound **Cu1** exhibited strong inhibitory potency against multiple oral planktonic bacteria and investigated its effects on *S.*

Table 3
Antibacterial activities of **Cu1** and chlorhexidine on multiple oral pathogens.

MIC (μg/mL)	<i>A. naeslundii</i> G ⁺	<i>S. gordonii</i> G ⁺	<i>S. sanguis</i> G ⁺	<i>A.a</i> G ⁻	<i>E. faecalis</i> G ⁺	<i>C. albicans</i> F	<i>L. casei</i> G ⁺	<i>F. nucleatum</i> G ⁻	<i>L. acidophilus</i> G ⁺
Cu1	0.49	0.98	1.95	1.95	3.91	3.91	15.63	31.25	31.25
Chlorhexidine	0.98	1.95	3.91	3.91	7.81	7.81	31.25	7.81	15.63

G⁺: gram-positive bacteria; G⁻: gram-negative bacteria; F: fungus.

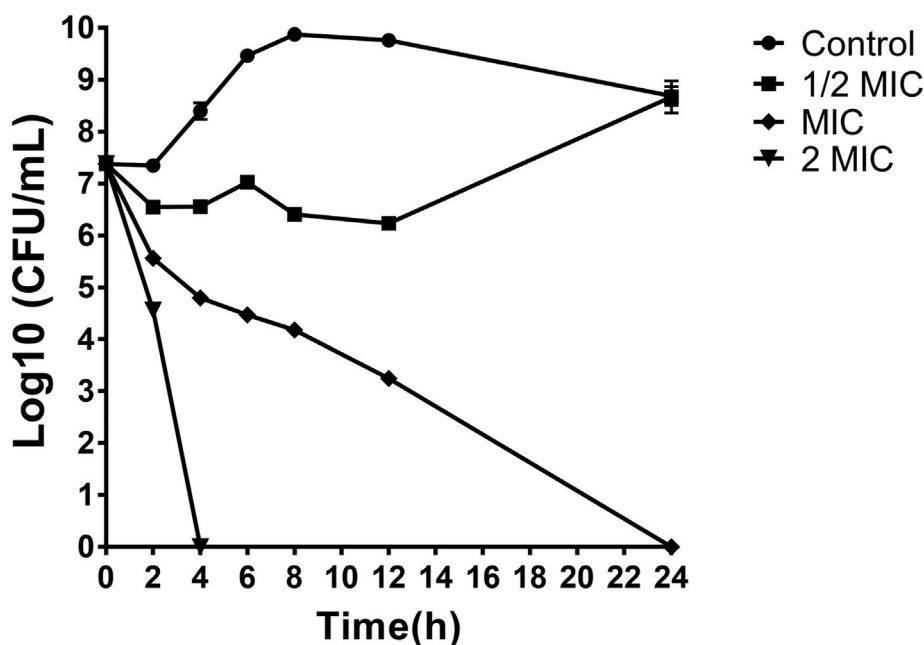


Fig. 2. The time-kill kinetics of **Cu1** against *S. mutans* UA159. The bacteria were treated at the concentrations of 1/2, 1, and 2 MIC. The pathogen untreated with compounds was selected as a control. The data are presented as the means ± SD.

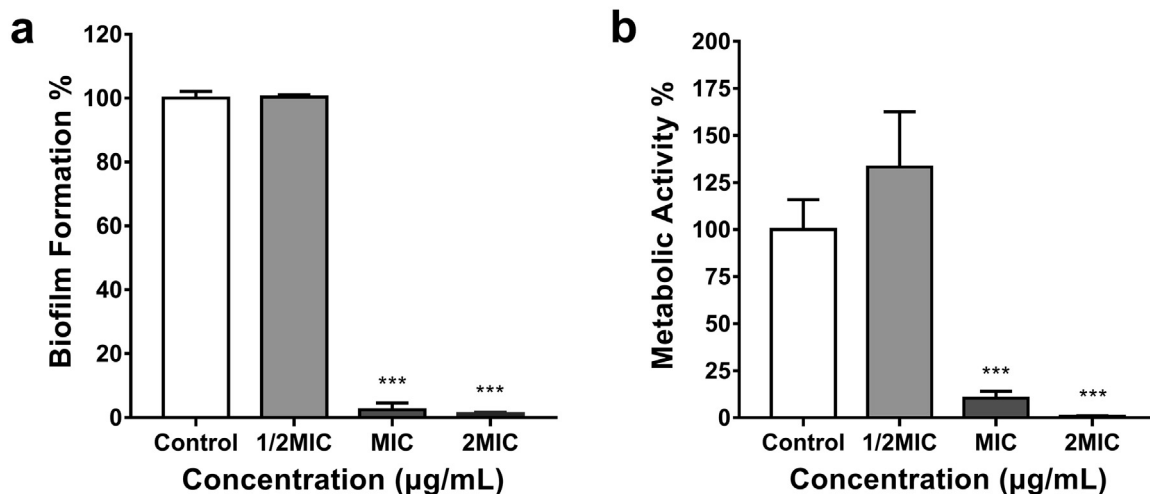


Fig. 3. The CV (a) and MTT (b) assays with **Cu1** against *S. mutans* UA159 biofilm formation after 24 h. The data are presented as the means ± SD. ****P* < 0.001, significant difference from the control group.

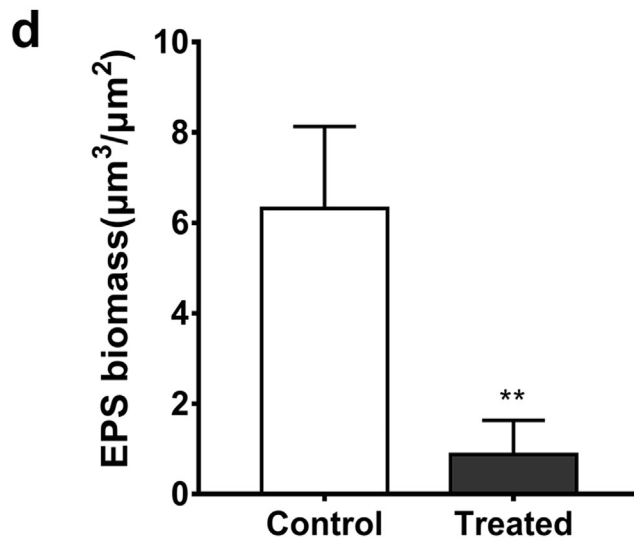
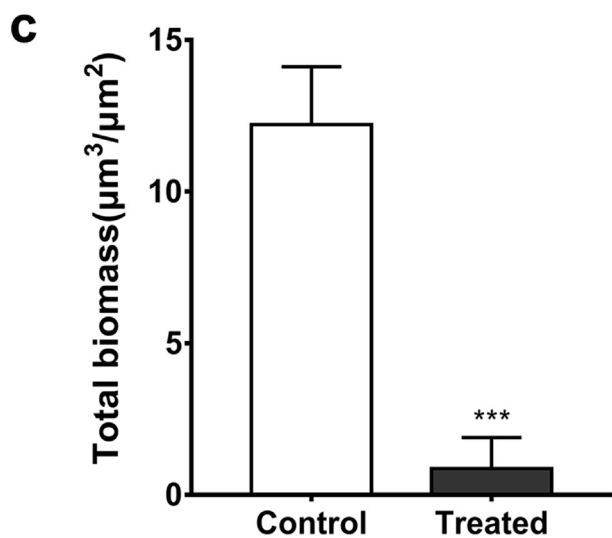
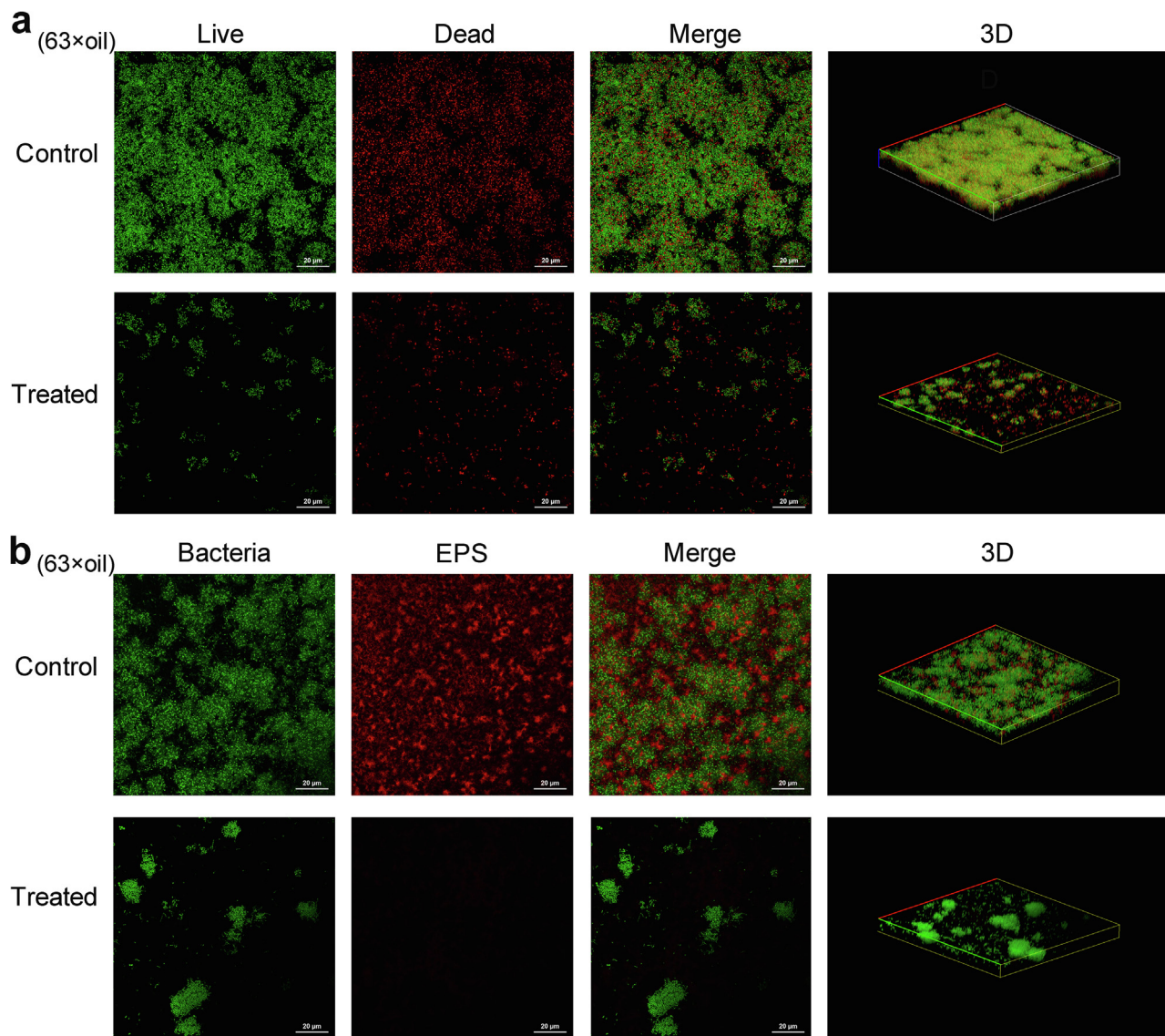


Fig. 4. CLSM images of *S. mutans* biofilms. Single, double channel and three-dimensional reconstructions of *S. mutans* biofilms in the control and treated groups. (a) Green reflects live bacteria and red reflects dead bacteria. (b) Green indicates microorganisms and red indicates EPS. (c) Quantitative analysis of the total bacterial biomass in (a). (d) Quantitative analysis of the EPS biomass in (b). The data are presented as the means \pm SD. *** $P < 0.01$; **** $P < 0.001$. (For interpretation of the references to colour in this figure legend, the reader is referred to the web version of this article.)

mutans biofilm formation. Comparatively, the bulkier, more sterically hindered NHC copper complexes **Cu2–Cu7** afforded much lower activity. Reasonably, the inhibitory properties are corrected with the structure of the copper-NHCs complexes. As depicted in the solid state of the X-ray structure, the *N*-moieties were found roughly perpendicular to the coordination plane, which suggests the axial steric effect derived from the 2,6-positions on the *N*-moieties would exert much repulsion from the copper centre, therefore retarding the flexibility of the coordination.

In addition to exploring the MIC values, a time-kill assay further confirmed that **Cu1** was bactericidal and sustained its inhibition and killing effects at the MIC as well as short-term and efficient eradication at twice this concentration. Moreover, **Cu1** was pivotal in the disruption of biofilm formation, even with a relatively high density of bacteria (2×10^7 CFU/mL), which was verified by a series of subsequent experiments. Accordingly, it is reasonable to speculate that the capacity of **Cu1** to affect biofilm formation is based on its bacterial cell killing effects.

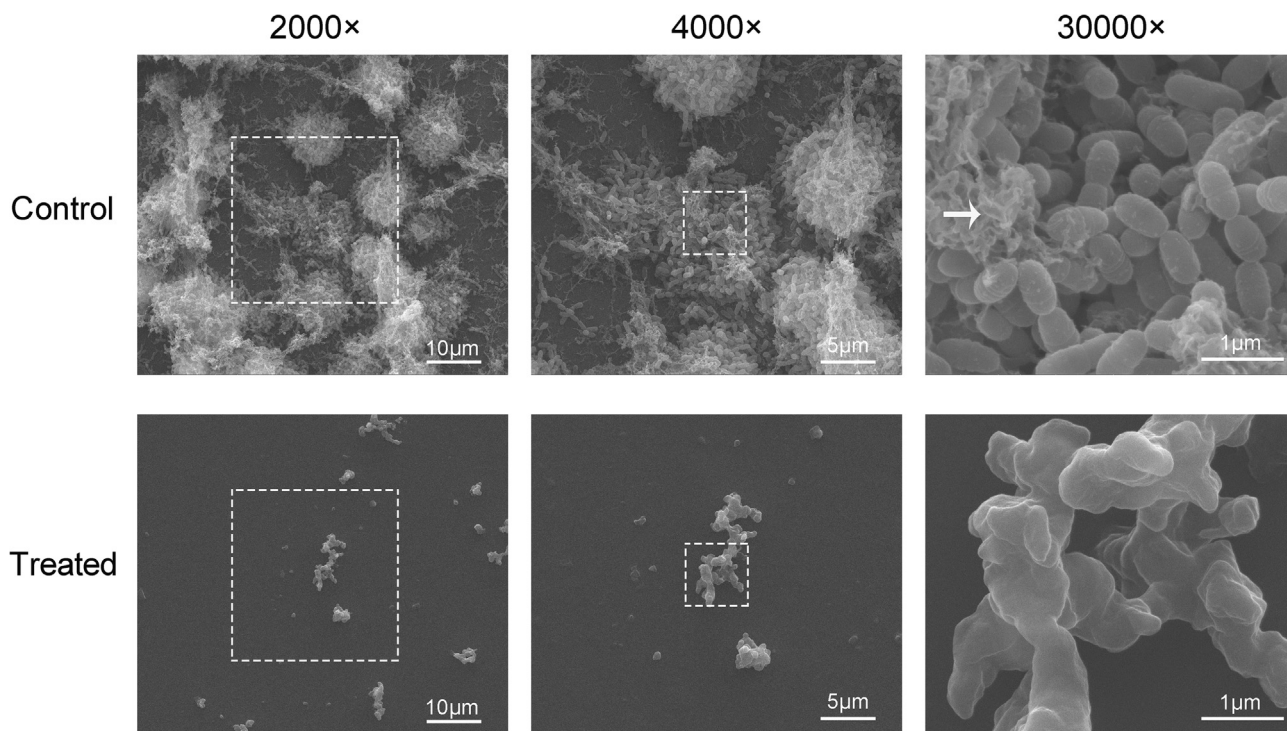


Fig. 5. Morphological changes in *S. mutans* biofilms with or without **Cu1** complex treatment. Each visual field is at 2000×, 4000× and 30,000× magnification. The boxes show enlarged areas. The white arrow indicates EPS in the biofilm. The black arrows indicate the different morphologies of *S. mutans*.

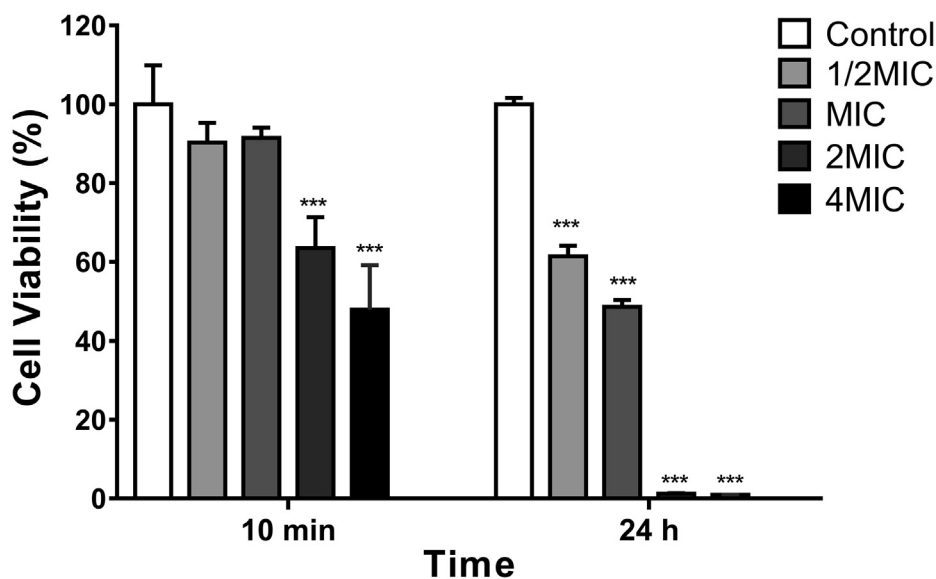


Fig. 6. Cytotoxicity of **Cu1** (0.49 µg/mL–7.81 µg/mL) on HGECs after 10 min and 24 h of incubation. The data are shown as the means ± SD. The asterisks (*) indicate the significant differences (***) $P < 0.001$.

The CV and MTT assays showed effective reductions in the biofilm biomass and metabolic activities by **Cu1** at the MIC. Combined with the results of the previous section, our conjecture was confirmed. This biofilm inhibition is most likely due to a reduction in the number of bacteria. Biofilm morphology observation experiments also confirmed this phenomenon.

EPS production, which directly mediates microbial adherence to a surface, forms a polymeric matrix that enhances the mechanical stability of biofilms [35]. Hence, EPS is recognized as one of the key virulence factors of oral biofilms in terms of the development of caries [58]. Both CLSM and SEM were used to assess the biofilm microstructure, and EPS production was strikingly reduced after **Cu1** treatment. This decrease in EPS production greatly contributed to preventing the formation of a three-dimensional biofilm structure. Moreover, microscopic studies showed that **Cu1** caused an altered biofilm phenotype, with a reduced number of cells. SEM also showed deformed, distorted, and collapsed cells, while the normal cell shape is a short rod. The altered cell morphology appears to be one of the major causes of deficient biofilms.

The biocompatibility of the newly synthesized molecule is an impediment for its clinical translation. These results demonstrated that short-duration treatment with **Cu1** below 1.95 µg/mL (MIC) did not have a negative impact on human oral cells, while long-term and high-dose exposure can affect cell activity. Actually, it has been observed that when **Cu1** is used as a mouthwash agent at this concentration for a short period of time, it can play a role in affecting the reproduction of *A. naeslundii*, *S. gordonii*, *S. sanguis*, *A. a* and *S. mutans*. **Cu1** has the characteristics of high activity and low cytotoxicity in a short-term treatment mode, making it a preferable agent for preventing dental caries. Copper-NHCs have been discovered as potential oral hygiene products.

5. Conclusion

In summary, a series of well-defined and air-stable copper-NHCs were synthesized and characterized. In the current research, we screened these complexes against *S. mutans* UA159. One of these complexes (**Cu1**) presented excellent performance with regards to the inhibition and killing of planktonic *S. mutans*, which suggested that less lipophilic and less sterically hindered copper complexes would be effective towards this bacteria. Compared with the traditional drug chlorhexidine, **Cu1** had a stronger antibacterial effect on a variety of oral pathogens (*Actinomyces naeslundii*, *Streptococcus gordonii*, *Streptococcus sanguis*, *Actinobacillus actinomycetemcomitans*, *Enterococcus faecalis*, *Candida albicans*, and *Lactobacillus casei*). **Cu1** also effectively inhibited *S. mutans* biofilm formation at its minimum inhibitory concentration. Moreover, **Cu1** showed good biocompatibility after short-term application.

CRedit authorship contribution statement

Ting Pan: Conceptualization, Methodology, Data curation, Formal analysis, Writing - original draft. **Yinuo Wang:** Software, Data curation, Formal analysis. **Feng-Shou Liu:** Resources. **Huancai Lin:** Writing - review & editing, Supervision, Project administration, Funding acquisition. **Yan Zhou:** Conceptualization, Writing - review & editing, Project administration, Funding acquisition.

Declaration of Competing Interest

The authors declare that they have no known competing financial interests or personal relationships that could have appeared to influence the work reported in this paper.

Acknowledgements

This work was supported by the Guangdong Financial Fund for High-Caliber Hospital Construction [grant number 174-2018-XMZC-0001-03-0125/-03] and by the Natural Science Foundation of Guangdong Province [grant number 2018A030313296].

Appendix A. Supplementary data

The CCDC contains the supplementary crystallographic data for **Cu5**. These data can be obtained free of charge via <http://www.ccdc.cam.ac.uk/conts/retrieving.html> or from the Cambridge Crystallographic Data Centre, 12 Union Road, Cambridge CB2 1EZ, UK; fax: (+44) 1223-336-033; or e-mail: deposit@ccdc.cam.ac.uk. Supplementary data to this article can be found online at <https://doi.org/10.1016/j.poly.2021.115033>.

References

- [1] A.J. Arduengo, R.L. Harlow, M. Kline, A stable crystalline carbene, *J. Am. Chem. Soc.* 22 (1991) 361–363.
- [2] G.C. Fortman, S.P. Nolan, N-Heterocyclic carbene (NHC) ligands and palladium in homogeneous cross-coupling catalysis: a perfect union, *Chem. Soc. Rev.* 40 (2011) 5151–5169.
- [3] M.N. Hopkinson, C. Richter, M. Schedler, F. Glorius, An overview of N-heterocyclic carbenes, *Nature* 510 (2014) 485–496.
- [4] M.L. Teyssot, A.S. Jarrousse, M. Manin, A. Chevry, S. Roche, F. Norre, C. Beaudoin, L. Morel, D. Boyer, R. Mahiou, A. Gautier, Metal-NHC complexes: a survey of anti-cancer properties, *Dalton Trans.* (2009) 6894–6902.
- [5] W. Liu, R. Gust, Metal N-heterocyclic carbene complexes as potential antitumor metallodrugs, *Chem. Soc. Rev.* 42 (2013) 755–773.
- [6] S.B. Aher, P.N. Muskawar, K. Thenmozhi, P.R. Bhagat, Recent developments of metal N-heterocyclic carbenes as anticancer agents, *Eur. J. Med. Chem.* 81 (2014) 408–419.
- [7] S.A. Patil, S.A. Patil, R. Patil, R.S. Keri, S. Budagumpi, G.R. Balakrishna, M. Tacke, N-heterocyclic carbene metal complexes as bio-organometallic antimicrobial and anticancer drugs, *Future Med. Chem.* 7 (2015) 1305–1333.
- [8] W.H. Zhao, V. Ferro, M.V. Baker, Carbohydrate-N-heterocyclic carbene metal complexes: synthesis, catalysis and biological studies, *Coord. Chem. Rev.* 339 (2017) 1–16.
- [9] S.Y. Hussaini, R.A. Haque, M.R. Razali, Recent progress in silver(I)-, gold(I)/(III)- and palladium(II)-N-heterocyclic carbene complexes: a review towards biological perspectives, *J. Organomet. Chem.* 882 (2019) 96–111.
- [10] O. Karaca, S.M. Meier-Menches, A. Casini, F.E. Kuhn, On the binding modes of metal NHC complexes with DNA secondary structures: implications for therapy and imaging, *Chem. Commun. (Camb.)* 53 (2017) 8249–8260.
- [11] W. Streciwilk, F. Hackenberg, H. Muller-Bunz, M. Tacke, Synthesis and cytotoxicity studies of p-benzyl substituted NHC-copper(I) bromide derivatives, *Polyhedron* 80 (2014) 3–9.
- [12] M.J. Matos, C. Labão-Almeida, C. Sayers, O. Dada, M. Tacke, G.J.L. Bernardes, Synthesis and biological evaluation of homogeneous thiol-linked NHC-Au-albumin and -trastuzumab bioconjugates, *Chem. Eur. J.* 24 (2018) 12250–12253.
- [13] A. Kascatan-Nebioglu, A. Melaiye, K. Hindi, S. Durmus, M.J. Panzner, L.A. Hogue, R.J. Mallett, C.E. Hovis, M. Coughenour, S.D. Crosby, A. Milsted, D.L. Ely, C.A. Tessier, C.L. Cannon, W.J. Youngs, Synthesis from caffeine of a mixed N-heterocyclic carbene-silver acetate complex active against resistant respiratory pathogens, *J. Med. Chem.* 49 (2006) 6811–6818.
- [14] S. Ray, R. Mohan, J.K. Singh, M.K. Samantaray, M.M. Shaikh, D. Panda, P. Ghosh, Anticancer and antimicrobial metallopharmaceutical agents based on palladium, gold, and silver N-heterocyclic carbene complexes, *J. Am. Chem. Soc.* 129 (2007) 15042–15053.
- [15] A. Pothig, S. Ahmed, H.C. Winther-Larsen, S. Guan, P.J. Altmann, J. Kudermann, A.M. Santos Andresen, T. Gjoen, O.A. Hogmoen Astrand, Antimicrobial Activity and cytotoxicity of Ag(I) and Au(I) pillarplexes, *Front. Chem.* 6 (2018) 584.
- [16] C.R. Shahini, G. Achar, S. Budagumpi, H. Muller-Bunz, M. Tacke, S.A. Patil, Benzoxazole and dioxolane substituted benzimidazole-based N-heterocyclic carbene-silver(I) complexes: synthesis, structural characterization and in vitro antimicrobial activity, *J. Organomet. Chem.* 868 (2018) 1–13.
- [17] P.O. Asekunowo, R.A. Hague, M.R. Razali, S.W. Avicor, M.F.F. Wajidi, Synthesis and characterization of nitrile functionalized silver(I)-N-heterocyclic carbene complexes: DNA binding, cleavage studies, antibacterial properties and mosquitocidal activity against the dengue vector, *Aedes albopictus*, *Eur. J. Med. Chem.* 150 (2018) 601–615.
- [18] A. Frei, J. Zuegg, A.G. Elliott, M. Baker, S. Braese, C. Brown, F. Chen, C.G. Dowson, G. Dujardin, N. Jung, A.P. King, A.M. Mansour, M. Massi, J. Moat, H.A. Mohamed, A.K. Renfrew, P.J. Rutledge, P.J. Sadler, M.H. Todd, C.E. Willans, J.J. Wilson, M.A. Cooper, M.A.T. Blaskovich, Metal complexes as a promising source for new antibiotics, *Chem. Sci.* 11 (2020) 2627–2639.

- [19] A. Kazancı, Y. Gök, R. Kaya, A. Aktaş, P. Taslimi, İ. Gülçin, Synthesis, characterization and bioactivities of dative donor ligand N-heterocyclic carbene (NHC) precursors and their Ag(I)/NHC coordination compounds, *Polyhedron* 193 (2021) 114866.
- [20] M.E. Garner, W.J. Niu, X.G. Chen, I. Ghiviriga, K.A. Abboud, W.H. Tan, A.S. Veige, N-heterocyclic carbene gold(I) and silver(I) complexes bearing functional groups for bio-conjugation, *Dalton Trans.* 44 (2015) 1914–1923.
- [21] C. Santini, M. Pellei, V. Gandin, M. Porchia, F. Tisato, C. Marzano, Advances in copper complexes as anticancer agents, *Chem. Rev.* 114 (2014) 815–862.
- [22] B. Bertrand, G. Gontard, C. Botuha, M. Salmain, Pincer-based heterobimetallic Pt(II)/Ru(II), Pt(II)/Ir(III), and Pt(II)/Cu(I) complexes: synthesis and evaluation of antiproliferative properties, *Eur. J. Inorg. Chem.* 2020 (2020) 3370–3377.
- [23] F. Lazreg, C.S.J. Cazin, Medical applications of NHC–gold and –copper complexes, *N-Heterocycl. Carbenes* (2014) 173–198.
- [24] M.L. Teyssot, A.S. Jarrouse, A. Chevy, A. De Haze, C. Beaudoin, M. Manin, S.P. Nolan, S. Diez-Gonzalez, L. Morel, A. Gautier, Toxicity of copper(I)-NHC complexes against human tumor cells: induction of cell cycle arrest, apoptosis, and DNA cleavage, *Chem. Eur. J.* 15 (2009) 314–318.
- [25] M. Vincent, P. Hartemann, M. Engels-Deutsch, Antimicrobial applications of copper, *Int. J. Hyg. Environ. Health* 219 (2016) 585–591.
- [26] D. Mitra, M. Li, E.T. Kang, K.G. Neoh, Transparent copper-based antibacterial coatings with enhanced efficacy against *Pseudomonas aeruginosa*, *ACS Appl. Mater. Interfaces* 11 (2019) 73–83.
- [27] J. Miguel-Avila, M. Tomas-Gamasa, A. Olmos, P.J. Perez, J.L. Mascarenas, Discrete Cu(I) complexes for azide-alkyne annulations of small molecules inside mammalian cells, *Chem. Sci.* 9 (2018) 1947–1952.
- [28] T. Bernardi, S. Badel, P. Mayer, J. Groelly, P. de Fremont, B. Jacques, P. Braunstein, M.L. Teyssot, C. Gaulier, F. Cisnetti, A. Gautier, S. Roland, High-throughput screening of metal-N-heterocyclic carbene complexes against biofilm formation by pathogenic bacteria, *ChemMedChem* 9 (2014) 1140–1144.
- [29] N. Touj, A. Chakchouk-Mtibaa, L. Mansour, A.H. Harrath, J. Al-Tamimi, L. Mellouli, I. Ozdemir, S. Yasar, N. Hamdi, Synthesis, spectroscopic properties and biological activity of new Cu(I) N-heterocyclic carbene complexes, *J. Mol. Struct.* 1181 (2019) 209–219.
- [30] N.B. Pitts, D.T. Zerov, P.D. Marsh, K. Ekstrand, J.A. Weintraub, F. Ramos-Gomez, J. Tagami, S. Twetman, G. Tsakos, A. Ismail, Dental caries, *Nat. Rev. Dis. Primers* 3 (2017) 17030.
- [31] R.H. Selwitz, A.I. Ismail, N.B. Pitts, Dental caries, *Lancet* 369 (2007) 51–59.
- [32] G.B.D. Disease, I. Injury, C. Prevalence, Global, regional, and national incidence, prevalence, and years lived with disability for 328 diseases and injuries for 195 countries, 1990–2016: a systematic analysis for the Global Burden of Disease Study 2016, *Lancet* 390 (2017) 1211–1259.
- [33] P.D. Marsh, Microbiology of dental plaque biofilms and their role in oral health and caries, *Dent. Clin. North Am.* 54 (2010) 441–454.
- [34] J.A. Banas, Virulence properties of *Streptococcus mutans*, *Front. Biosci.* 9 (2004) 1267–1277.
- [35] W.H. Bowen, R.A. Burne, H. Wu, H. Koo, Oral biofilms: pathogens, matrix, and polymicrobial interactions in microenvironments, *Trends Microbiol.* 26 (2018) 229–242.
- [36] X.-B. Lan, F.-M. Chen, B.-B. Ma, D.-S. Shen, F.-S. Liu, Pd-PEPPSI Complexes Bearing Bulky [(1,2-Di-(tert-butyl)acenaphthyl)] (DtBu-An) on N-heterocarbene backbones: highly efficient for Suzuki-Miyaura Cross-Coupling Under Aerobic Conditions, *Organometallics* 35 (2016) 3852–3860.
- [37] X.X. He, Y.W. Li, B.B. Ma, Z.F. Ke, F.S. Liu, Sterically encumbered tetraarylimidazolium carbene Pd-PEPPSI complexes: highly efficient direct arylation of imidazoles with aryl bromides under aerobic conditions, *Organometallics* 35 (2016) 2655–2663.
- [38] X.B. Lan, Y. Li, Y.F. Li, D.S. Shen, Z. Ke, F.S. Liu, Flexible steric bulky bis(imino)acenaphthene (BIAN)-supported N-heterocyclic carbene palladium precatalysts: catalytic application in Buchwald-Hartwig amination in air, *J. Org. Chem.* 82 (2017) 2914–2925.
- [39] D.D. Lu, X.X. He, F.S. Liu, Bulky yet flexible Pd-PEPPSI-IPent(An) for the synthesis of sterically hindered biaryls in air, *J. Org. Chem.* 82 (2017) 10898–10911.
- [40] L.Q. Hu, R.L. Deng, Y.F. Li, C.J. Zeng, D.S. Shen, F.S. Liu, Developing bis(imino)acenaphthene-supported N-heterocyclic carbene palladium precatalysts for direct arylation of azoles, *Organometallics* 37 (2018) 214–226.
- [41] J.S. Ouyang, Y.F. Li, F.D. Huang, D.D. Lu, F.S. Liu, The highly efficient Suzuki-Miyaura cross-coupling of (Hetero)aryl chlorides and (hetero)arylboronic acids catalyzed by “bulky-yet-flexible” palladium-PEPPSI complexes in air, *ChemCatChem* 10 (2018) 371–375.
- [42] F.D. Huang, C. Xu, D.D. Lu, D.S. Shen, T. Li, F.S. Liu, Pd-PEPPSI-IPent(An) promoted deactivated amination of aryl chlorides with amines under aerobic conditions, *J. Org. Chem.* 83 (2018) 9144–9155.
- [43] D.H. Li, X.X. He, C. Xu, F.D. Huang, N. Liu, D.S. Shen, F.S. Liu, N-heterocarbene palladium complexes with dianisole backbones: synthesis, structure, and catalysis, *Organometallics* 38 (2019) 2539–2552.
- [44] F.Y. Zhang, X.B. Lan, C. Xu, H.G. Yao, T. Li, F.S. Liu, Rigid hindered N-heterocyclic carbene palladium precatalysts: synthesis, characterization and catalytic amination, *Org. Chem. Front.* 6 (2019) 3292–3299.
- [45] X.W. Yang, D.H. Li, A.X. Song, F.S. Liu, “Bulky-yet-flexible” alpha-diimine palladium-catalyzed reductive heck cross-coupling: highly anti-Markovnikov-selective hydroarylation of alkene in air, *J. Org. Chem.* 85 (2020) 11750–11765.
- [46] C. Chen, F.S. Liu, M. Szostak, BIAN-NHC ligands in transition-metal-catalysis: a perfect union of sterically-encumbered, electronically-tunable N-heterocyclic carbenes?, *Chem. Eur. J.* (2020), <https://doi.org/10.1002/chem.202003923>.
- [47] O. Santoro, A. Collado, A.M. Slawin, S.P. Nolan, C.S. Cazin, A general synthetic route to [Cu(X)(NHC)] (NHC = N-heterocyclic carbene, X = Cl, Br, I) complexes, *Chem. Commun. (Camb.)* 49 (2013) 10483–10485.
- [48] C.A. Citadelle, E. Le Nouy, F. Bisaro, A.M. Slawin, C.S. Cazin, Simple and versatile synthesis of copper and silver N-heterocyclic carbene complexes in water or organic solvents, *Dalton Trans.* 39 (2010) 4489–4491.
- [49] Ca.L.S. Institute, Performance Standards for Antimicrobial Susceptibility Testing; Twenty-Second Informational Supplement CLSI Document M100-S22, 2012.
- [50] J. Xiao, M.I. Klein, M.L. Falsetta, B. Lu, C.M. Delahunty, J.R. Yates 3rd, A. Heydorn, H. Koo, The exopolysaccharide matrix modulates the interaction between 3D architecture and virulence of a mixed-species oral biofilm, *PLoS Pathog.* 8 (2012) e1002623.
- [51] H. Kaur, F.K. Zinn, E.D. Stevens, S.P. Nolan, (NHC)Cu-I (NHC = N-heterocyclic carbene) complexes as efficient catalysts for the reduction of carbonyl compounds, *Organometallics* 23 (2004) 1157–1160.
- [52] P. Shaw, A.R. Kennedy, D.J. Nelson, Synthesis and characterisation of an N-heterocyclic carbene with spatially-defined steric impact, *Dalton Trans.* 45 (2016) 11772–11780.
- [53] A.G. Dalecki, C.L. Crawford, F. Wolschendorf, Copper and antibiotics: discovery, modes of action, and opportunities for medicinal applications, *Adv. Microb. Physiol.* 70 (2017) 193–260.
- [54] M. Tegoni, D. Valensin, L. Toso, M. Remelli, Copper chelators: chemical properties and bio-medical applications, *Curr. Med. Chem.* 21 (2014) 3785–3818.
- [55] L. Macomber, J.A. Imlay, The iron-sulfur clusters of dehydratases are primary intracellular targets of copper toxicity, *Proc. Natl. Acad. Sci. U.S.A.* 106 (2009) 8344–8349.
- [56] S. Tottey, C.J. Patterson, L. Banci, I. Bertini, I.C. Felli, A. Pavelkova, S.J. Dainty, R. Pernil, K.J. Waldron, A.W. Foster, N.J. Robinson, Cyanobacterial metallochaperone inhibits deleterious side reactions of copper, *Proc. Natl. Acad. Sci. U.S.A.* 109 (2012) 95–100.
- [57] I. Iakovidis, I. Delimaris, S.M. Piperakis, Copper and its complexes in medicine: a biochemical approach, *Mol. Biol. Int.* 2011 (2011) 594529.
- [58] H. Koo, J. Xiao, M.I. Klein, Extracellular polysaccharides matrix – an often forgotten virulence factor in oral biofilm research, *Int. J. Oral Sci.* 1 (2009) 229–234.